FERROBORON PRODUCTION BY ELECTRODEOXIDATION

A THESIS SUBMITTED TO
THE GRADUATE SCHOOL OF NATURAL AND APPLIED SCIENCES
OF
MIDDLE EAST TECHNICAL UNIVERSITY

BY

TAYLAN ÖRS

IN PARTIAL FULFILLMENT OF THE REQUIREMENTS
FOR
THE DEGREE OF MASTER OF SCIENCE
IN
METALLURGICAL AND MATERIALS ENGINEERING

SEPTEMBER 2008

Approval of the thesis:

FERROBORON PRODUCTION BY ELECTRODEOXIDATION

Submitted by **TAYLAN ÖRS** in partial fulfillment of the requirements for the degree of **Master of Science in Metallurgical and Materials Engineering, Middle East Technical University** by,

Prof. Dr. Canan Özgen _____
Dean, Graduate School of **Natural and Applied Sciences**

Prof. Dr. Tayfur Öztürk _____
Head of Department, **Metallurgical and Materials Engineering, METU**

Prof. Dr. Tayfur Öztürk _____
Supervisor, **Metallurgical and Materials Engineering, METU**

Prof. Dr. İshak Karakaya _____
Co-Supervisor, **Metallurgical and Materials Engineering, METU**

Examining Committee Members:

Prof. Dr. Naci Sevinç _____
Metallurgical and Materials Engineering, METU

Prof. Dr. Tayfur Öztürk _____
Metallurgical and Materials Engineering, METU

Prof. Dr. İshak Karakaya _____
Metallurgical and Materials Engineering, METU

Erk İnger _____
General Manager, BOREN

Prof. Dr. C. Hakan Gür _____
Metallurgical and Materials Engineering, METU

04.09.2008

I hereby declare that all information in this document has been obtained and presented in accordance with academic rules and ethical conduct. I also declare that, as required by these rules and conduct, I have fully cited and referenced all material and results that are not original to this work.

TAYLAN ÖRS

ABSTRACT

FERROBORON PRODUCTION BY ELECTRODEOXIDATION

Örs, Taylan

M.Sc., Department of Metallurgical and Materials Engineering

Supervisor : Prof. Dr. Tayfur Öztürk

Co-supervisor: Prof. Dr. İshak Karakaya

September 2008, 44 pages

In this study ferroboron (Fe - 14 at %B) was synthesized in crystalline form (Fe + Fe_2B) via electrodeoxidation. For this purpose, Fe_2O_3 and H_3BO_3 were mixed in suitable proportions via spex mill. The powder was cold pressed and sintered at 900 $^{\circ}$C yielding a two phase structure Fe_3BO_6 and Fe_2O_3. The sintered pellets were electro-deoxidized in $CaCl_2$ by applying 3.1 Volts at 850°C for 12 hours. This yielded Fe and Fe_2B in proportions slightly deviating from the target composition. The chemical pathway of reduction is inspected by the help of the available thermodynamic data and the x-ray characterization of partially reduced samples. CaO and the formation of $Ca_3B_2O_6$ were found to be effective in the mid-steps of this electrodeoxidation process.

Keywords: Electrodeoxidation, Ferroboron, Molten Salt, B_2O_3

ÖZ

FERROBORUN ELEKTRODEOKSİDASYON İLE ÜRETİMİ

Örs, Taylan

Yüksek Lisans, Metalurji ve Malzeme Mühendisliği Bölümü
Tez Yöneticisi : Prof. Dr. Tayfur Öztürk
Yardımcı Tez Yöneticisi: Prof. Dr. İshak Karakaya

Eylül 2008, 44 sayfa

Bu çalışmada ferrobor (Fe -% at 14 B) kristal halde (Fe + Fe_2B) elektrodeoksidasyon ile sentezlenmiştir. Bunun için Fe_2O_3 ve H_3BO_3 gereken oranlarda spex öğütücüsünde karıştırılmıştır. Oluşan toz soğuk preslenip ve 900°C'de sinterlenmiştir ve bunun sonusunda iki fazlı bir yapı elde edilmiştir (Fe_3BO_6 ve Fe_2O_3). Sinterlenmiş pelletler $CaCl_2$ içerisinde 850°C'de 3.1 V gerilim uygulanarak 12 saat boyunca elektrodeoksidasyon işlemine tabi tutulmuştur. İşlem sonucunda yapıda hedef kompozisyondan bir miktar fark gösteren oranlarda Fe ve Fe_2B bulunmuştur. İndirgenme işleminin kimyasal mekanizması mevcut termodinamik veri ve kısmen indirgenen numunelerin x-ışınları analizi yardımı ile incelenmiştir. CaO ve $Ca_3B_2O_6$ bileşiklerinin elektrodeoksidasyon işleminin ara basamaklarında etkili olduğu tespit edilmiştir.

Anahtar Kelimeler: Elektrodeoksidasyon, Ferrobor, Erimiş Tuz, B_2O_3

ACKNOWLEDGEMENTS

I wish to express my deepest gratitude to my supervisor Prof. Dr. Tayfur Öztürk, cosupervisor Prof. İshak Karakaya, Prof. Dr. Kadri Aydınol and Mr. Serdar Tan for their guidance, advice, criticism, encouragements and insight throughout the research.

I would also like to thank Prof. Dr. Bilgehan Ögel for permitting the use of the facilities in his laboratory. Thanks go to all of my research group members and friends in the Metallurgical and Materials Engineering Department for their help and support.

The technical assistance of Mr.Cengiz Tan and Mr. Cemal Yanardağ are gratefully acknowledged.

Finally I would like to thank to my family members, especially my sister Evrim Örs for their continuous support and patience.

This study was supported by the Scientific Research Council of Turkey (TÜBİTAK) Project No: MAG 105M352

TABLE OF CONTENTS

CHAPTER 1

INTRODUCTION

Most metals and some metalloids (such as B and Si) exist as oxides in nature due to their low affinity for electrons when compared to oxygen atom. For engineering purposes however, the oxide materials are not always desirable – they are mostly brittle, electrically non-conducting, and unreliable. It is, therefore, essential to reduce these substances to yield metals and alloys. For this reason, vast amount of techniques have been developed in order to produce the elemental forms of these metals and metalloids from their oxides.

Electrochemical routes for reducing and refining metals in molten salts are known for more than a century. The earliest examples are molten salt electrolysis processes like Hall-Héroult process for aluminum production. According to this method, metal ions deposit at the cathode and the non-metallic component of the compound to be reduced is discharged at anode.

Solid state electrodeoxidation method is an electrochemical route to deoxidize appropriate metal oxide systems and allows formation of alloys and compounds in a more direct way. The process was first proposed by Fray et al. (1999) and is known as FFC (Fray-Farthing-Chen) Cambridge process. The method is similar to molten salt electrolysis except for the fact that the electrolyte neither decomposes

nor reduces the oxide material directly. In this process the oxide used as a cathode is gradually deoxidized first by ionizing the oxygen which dissolves in the electrolyte and is discharged from graphite anode in the form of CO or CO_2. The electrolytes in this process are usually molten salts of I A or II A group elements which has sufficient solubility for oxygen.

Besides reducing and refining metals, this technology offers a new prospect of reducing mixed oxide precursors to the final alloy of the respective metals. This feature of the process may open up a new era for some alloys that are difficult to produce by conventional methods. Figure 1 visualizes the difference between the current method and the conventional method of alloy production. As made clear by the figure, alloy production by electrodeoxidation process shortcuts a number of processes in the conventional route. Owing to this technology, once the ores of desired metals are converted to the oxides and blended, they are ready to be reduced, refined and alloyed in one single step. Details of this process and alloy production with this method will be discussed in the next chapter.

Ferroboron near the eutectic (Fe - 17 at % B) composition is an interesting alloy due to its glass forming ability. According to Inoue et al. (1997), this alloy when cooled down from the liquid phase will tend to yield an amorphous structure. Ferroboron when alloyed with elements like Co, Zr, Mo will tend to form amorphous structure more easily when the eutectic reaction is suppressed upon cooling, as reported by Akdeniz et al. (2005). These alloys in amorphous form have superior high electrical resistivity and good soft magnetic properties such as high saturation magnetization (MS), low coercive fields (HC), low core losses, and high magnetic permeabilities (μe), (McHenry et al. 1999). The alloy as such has a potential to replace Fe - Si alloys in the field of transformer core applications.

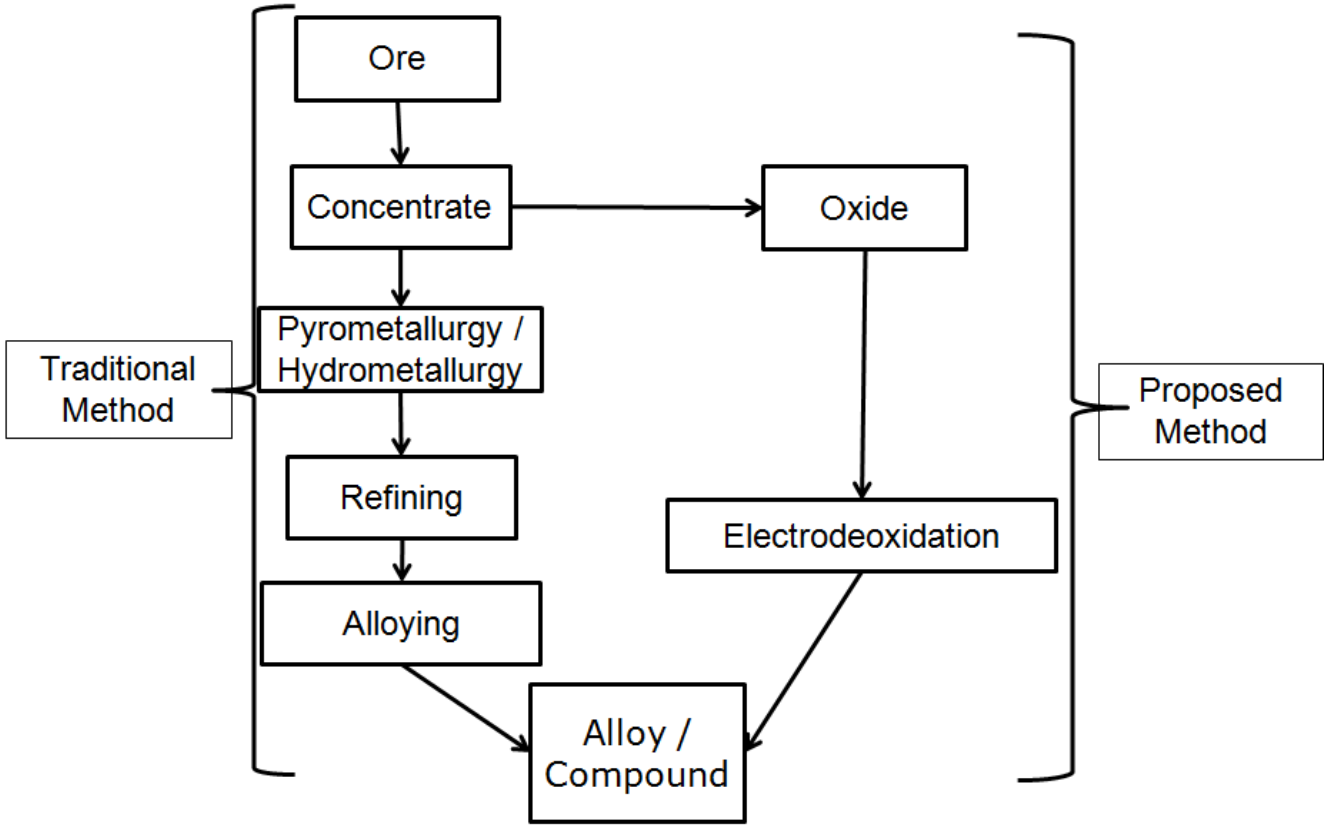

Figure 1: Schematic comparison between traditional method of alloy production with the proposed method (electrodeoxidation).

Fe-B compounds in crystalline form are also useful as coatings for its high hardness and wear resistance. As reported by Martini et al. (2004) Fe_2B and FeB polyphase coatings can be produced on iron or medium carbon steel so as to improve its wear properties.

The present study investigates ferroboron production directly from their oxides with the use of electrodeoxidation process. It may be mentioned that the conventional route for ferroboron production is by carbothermic reduction of boric acid with coke powder in presence of low carbon steels. An aluminothermic method is also suggested by Yücel et al. (1996).

CHAPTER 2

LITERATURE REVIEW

2.1 Electrodeoxidation Process

One of the most common and earliest examples of molten salt involving reduction procedure is the Hall-Héroult process for the production of Al from alumina, Al_2O_3. According to this process, Al_2O_3 is dissolved in molten cryolite Na_3AlF_6. When this mixture is electrolyzed, oxygen in alumina is discharged from the carbon anode (as CO or CO_2) and the metallic aluminum is deposited onto the cathode. This process is still regarded as the only commercial molten salt electrolysis process involving oxides.

Ward and Hoar (1961) were first to discover the removal of non-metallic (O, S, Se and Te) impurities from Cu by cathodic refining. The refining was done in molten $BaCl_2$ electrolyte and a current above the decomposition potential of the $BaCl_2$ was applied between graphite anode and impure Cu cathode. The impurities from the cathode are then discharged by the help of the applied current leaving pure Cu at the cathode. The proposed mechanism was the decomposition of $BaCl_2$ after which the deposited Ba could react with the impurities at the cathode. The overall reaction given by Mohandas and Fray (2004) for this procedure is:

$$Cu_2X + BaCl_2 = 2\ Cu + BaX + Cl_2 \qquad (1.1)$$

where X is O, S, or Se.

Following a similar idea, Okabe et al. (1992) describe a new process of reducing Ti from TiO_2 in a bath of molten $CaCl_2$ which is saturated with Ca. It is claimed that the Ca dissolved in the electrolyte reduces TiO_2 by calciothermic reduction and yields Ti with CaO as side product. This CaO is then electrolyzed in molten salt to refresh the reductant Ca^{2+} concentration in the electrolyte.

A recently invented process, FFC Cambridge process, which is proposed by Fray et al in late 90's (Fray et al. 1999), is schematically represented in Figure 2. Being similar to the cathodic refining procedure this method also allows reduction of the oxides to metals. It is simply a reduction process in the solid state where the oxides connected as cathode are electrolyzed in a molten salt against a graphite anode. In the process, the oxygen in the cathode is ionized, dissolved in the electrolyte and discharged from the anode in the form of CO_2 and/or CO leaving behind the metallic constituents. Method proposed by Fray et al. is different from cathodic refining in that the voltage applied is lower than the decomposition potential of the chloride salt. The method is claimed to be different from the method proposed by Okabe et al. (1992) in that there is no Ca metal dissolved in the molten salt, thereby eliminating the role of cation of the salt (Ba in $BaCl_2$, Ca in $CaCl_2$) in the process. This means that the deoxygenation and deoxidation carried out during the FFC process is not a result of calciothermic reduction, calcium deposition at the cathode or CaO formation. FFC process therefore introduces a new concept of cathodic oxygen ionization in which the oxygen (or any other anodic impurity) leaves the cathode by the reactions (Mohandas and Fray 2004):

$$X + 2\,e^- = X^{2-} \text{ (cathodic reaction)} \quad (1.2)$$

$$X^{2-} = X + 2e^- \text{ (anodic reaction)} \quad (1.3)$$

where X is O or another anodic impurity.

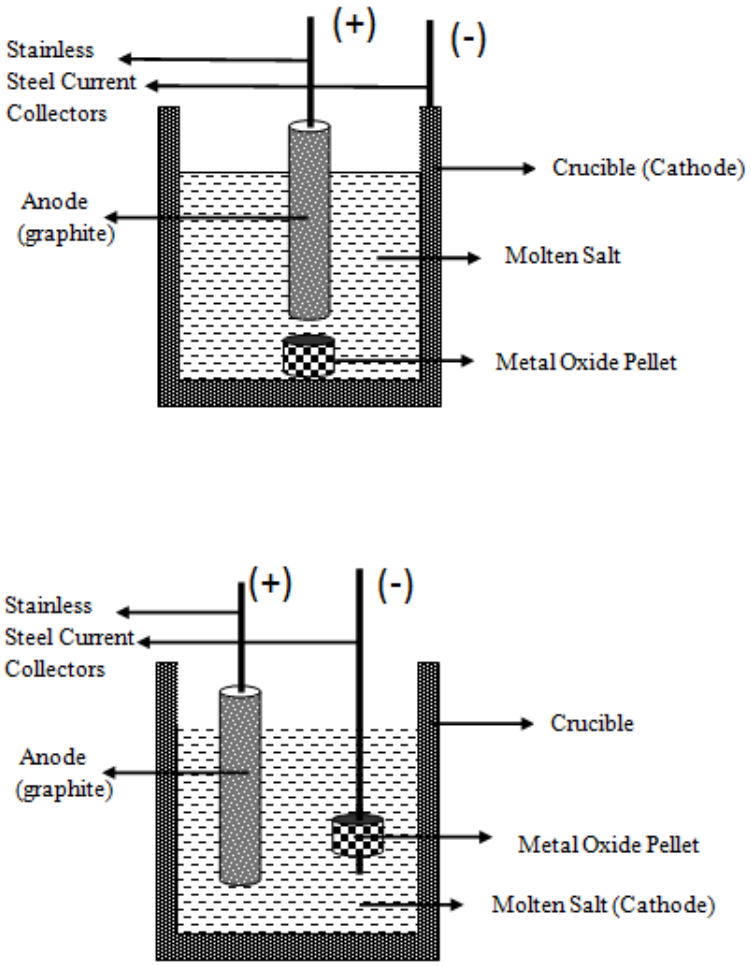

Figure 2: Two different cell designs for FFC Cambridge Process (Schematic). In the upper figure crucible is used as the cathode current collector and the sample is contacting to the crucible, whereas in the lower one the oxide sample to be reduced is attached to a stainless steel current collector and the crucible is a non-conducting material. (Adapted from Fray and Chen (2004))

The method proposed by Fray et al. differs from the molten salt electrolysis. As in Hall-Héroult process, in a typical molten salt process, the oxide to be reduced should be dissolved ionically in a liquid electrolyte and the electrolyte should subsequently be electrolyzed to reduce the desired metal. In the

electrodeoxidation (FFC Cambridge process) reduction mainly takes place in the solid oxide cathode and the molten chloride remains intact without decomposing.

The method of electrodeoxidation was originally developed for extraction of Ti from TiO_2 (Chen et al. 2000), but has been found suitable for most systems of the transition metal oxides or multivalent metal oxides. Basically, the principle is to remove chemically or physically bound oxygen by applying a voltage difference between the metal oxide (cathode) and the anode material (graphite or an inert metal). The oxide pellet on the cathode side will conduct electricity (by a complex mechanism the details of which are discussed by Schwandt et al. (2005)) and oxygen will ionize and dissolve in the fused salt. It will then be transported to the anode by diffusion under the applied electric field. The simplified reactions according to Mohandas and Fray (2004):

Cathode: $TiO_2 + 4e^- = Ti + 2O^{2-}$ (1.4)

Anode: $2O^{2-} + C = CO_2 + 4e^-$ (1.5)

Overall: $TiO_2 + C = Ti + CO_2$ (1.6)

The above reactions are also verified by X-ray analysis of the partially reduced oxides by Schwandt et al. (2005) and voltammetric studies by Chen et al. (2002).

2.2 Electrodeoxidation of Pure Oxides

This method is obviously not limited to titanium production, though TiO_2 is referred as the most suitable compound for reduction. Other oxides that are shown to be reduced are Nb_2O_5 (Yan and Fray 2002), Cr_2O_3 (Gordo et al. 2004), SnO_2 (Glowacki et al. 2003) NiO (Tan et al. 2007) and SiO_2 (Jin et al. 2004).

Yan and Fray (2002) used a eutectic melt of dehydrated $CaCl_2$-NaCl as the electrolyte for Nb_2O_5 reduction. The electrolysis was carried out at 900°C and the voltage applied was 3.1 V during the 48-hour experiment. Graphite was used as anode in this experiment. Nb_2O_5 oxide pellets were sintered at three different temperatures (900°C, 1100°C and 1300°C). Increasing the sintering temperature decreased the porosity of the pellets and slowed down the kinetics of reduction. They also noted that increased local activity of CaO in the melt caused various calcium niobates to form which is said to cause the reduction to slow down by inhibiting the expected pathway for reduction. The intermediate reaction products were niobium oxides and calcium niobates both of which are becoming more oxygen deficient as the deoxidation proceeds finally reaching to pure Nb.

Similar to Nb reduction, pellets sintered at different temperatures were used in Cr_2O_3 reduction by Gordo et al. (2004), varying from 900°C to 1450°C. In this detailed study, Cr_2O_3 has been reduced to Cr in both pure $CaCl_2$ and NaCl-$CaCl_2$ eutectic composition at temperatures varying from 600°C to 950°C. Electrolysis time was typically 4 hours where the constant cell voltage ranged from 2.8 V to 3.3 V. The results indicated that, the reduction in the samples sintered at lower temperatures were more complete. This was attributed to small particle sizes which are associated with low sintering temperatures. As stated in the same paper, increasing particle size increases the pathway of oxygen diffusion in the solid environment which is probably one of the slowest steps involved in the reduction process. Increasing the cell voltage from 2.8 V to 3.3 V resulted in the decrease of oxygen content; however current efficiencies were also decreased. Finally a study on the effects of the electrolysis temperature was carried out for temperatures between 600°C and 950°C in which the higher electrolysis temperatures were found to be more effective in reducing the oxide pellet.

SnO_2 was first electro-deoxidized by Glowacki et al. (2003). In this study SnO_2 was reduced for 10 hours at 900°C in a $CaCl_2$-NaCl eutectic melt which is

dehydrated prior to electrodeoxidation procedure. Anode material was graphite and the applied constant potential was 3.1 V. The proposed cathodic reactions are as follows:

$$3SnO_2 + 4e^- = Sn_3O_4 + 2O^{2-} \quad (1.7)$$

$$Sn_3O_4 + 2e^- = 3SnO + O^{2-} \quad (1.8)$$

$$SnO + 2e- = Sn\ (l) + O^{2-} \quad (1.9)$$

or:

$$SnO_2 + 2e^- = SnO + O^{2-} \quad (1.10)$$

$$SnO + 2e- = Sn\ (l) + O^{2-} \quad (1.11)$$

The reduction of Ni from NiO was studied by Tan et al. (2007). Experiments were performed at 900°C which have shown that NiO can be reduced successfully to Ni at times shorter than 17 hours.

The reduction of Si from SiO_2 was studied by Jin et al. (2004). SiO_2 powder was reduced to pure silicon in 4 hours and at 850°C. The electrolyte used was pure $CaCl_2$ and a constant voltage of 2.8 V is applied. The electrical conductivity of SiO_2 was discussed and a three-phase boundary model was proposed which was developed further in Deng et al. (2005). According to this model, reduction starts from the W (current collector) / SiO_2 / $CaCl_2$ interface and proceeds from the surface of the pellet until complete metallization of the surface of the oxide pellet. After that, the reduction takes place in the deeper regions of the pellet which could make contact with the liquid $CaCl_2$ through the porous solid silicon.

The decomposition potentials of the above mentioned oxides and $CaCl_2$ at 900°C have been calculated and are shown in Table 1. As seen from the table, the

carbothermic decomposition potentials of all these oxides are significantly lower than the reduction potential of $CaCl_2$. The reduction reactions and mechanisms proposed above are therefore thermodynamically favorable.

Electrodeoxidation method can be applied to all the metals and metalloids having their oxides less stable than $CaCl_2$ when subjected to carbothermic reduction. Muir-wood et al. (2003), point out the following reactions as the general pathway for reduction:

Cathode:

$$M_xO_y + 2ye^- = xM + yO^{2-} \quad (1.12)$$

Anode:

$$2O^{2-} = O_2 + 4e^- \quad (1.13)$$

$$O^{2-} + C = CO + 2e^- \quad (1.14)$$

$$2O^{2-} + C = CO_2 + 4e^- \quad (1.15)$$

Overall:

$$M_xO_y + zC = xM + (y-3)/2\ O_2 + CO + CO_2 \quad (1.16)$$

It should be pointed out that these reactions can alter slightly by the formation and decomposition of various calcium oxide containing compounds, as mentioned above.

Table 1: Decomposition potentials of various oxides and $CaCl_2$ at 900°C (Thermodynamic values are calculated from data obtained from Barin et al.1973).

Reduction Reactions	ΔG° at 900°C in Joules	No. of Electrons Transferred	Decomposition Potential at 900°C in Volts
$CaCl_2 = Ca + Cl_2$	619997	2	3,21
$TiO_2 + 2\ C = Ti + 2\ CO$	302743	4	1,57
$Cr_2O_3 + 3\ C = 2\ Cr + 3\ CO$	178653,1	6	0,93
$Nb_2O_5 + 5\ C = 2\ Nb + 5\ CO$	315765,4	10	1,64
$SnO_2 + 2\ C = Sn + 2\ CO$	-91302,7	4	-0,47
$SiO_2 + 2\ C = Si + 2\ CO$	270501,1	4	1,40
$NiO + C = Ni + CO$	-80347,1	2	-0,42

2.3 Electrodeoxidation of Mixed Oxides

One of the immediate advantages that the electrodeoxidation technology provides is the chance to produce alloys from a mixture of oxides directly. As shown in Figure 1 preparation of alloys with this method is much easier than conventional methods of alloy preparation because of the steps that are eliminated. In the conventional methods, the steps involving reduction and alloying are done separately whereas the electrodeoxidation process unites these steps in one single step. Many alloys have so far been produced by this method proves the advantage of this technology. Same route is still valid even if the final product is an intermetallic compound rather than an alloy.

Several alloys and intermetallic compounds have been prepared. Ni_2MnGa (Muir Wood et al. 2003), Nb_3Sn (Glowacki et al. 2003), $TbFe_2$ (Qiu et al. 2006), $TbNi_5$ (Qiu et al. 2006) and FeTi (Tan et al. 2007) are all shown to be produced by electrodeoxidation.

First compound reported in detail was Ni_2MnGa by Muir Wood et al. (2003). The mixed oxide powders (NiO, MnO_2 and Ga_2O_3) were sintered at 540°C. The oxide

compact produced were electrolyzed in pure $CaCl_2$ at 900°C with an applied voltage of 3.0 V. Deoxidation procedure lasted 26 h and the product was reported to be pure Ni_2MnGa.

Superconducting Nb_3Sn powders were synthesized via electrodeoxidation by Glowacki et al. (2003). The oxide pellets consisted of Nb_2O_5-SnO_2 mixture sintered at 935°C were electrolyzed in pre-dehydrated $CaCl_2$ - NaCl eutectic mixture for 10 hours. The molten salt temperature was 900°C and the potential applied was 3.1 V. The experiment yielded Nb_3Sn intermetallic. SnO_2 reduction mechanisms were as given above and the mechanism given for Nb_2O_5 reduction was quite similar.

Qiu et al. (2006), in their study on $TbFe_2$ production, have successfully reduced a blend of Tb_4O_7-Fe_2O_3 (sintered at different temperatures) in pure anhydrous $CaCl_2$ at 900°C. Two different voltages were applied with one being 2.6 V and the other 3.1 V. The proposed mechanism for reduction is:

$$Fe_2O_3 + 6\ e^- = 2\ Fe + 3\ O^{2-} \quad (1.17)$$

$$17\ Fe + Tb_2O_3 + 6\ e^- = Tb_2Fe_{17} + 3\ O^{2-} \quad (1.18)$$

$$6\ Tb_2Fe_{17} + 11\ Tb_2O_3 + 66\ e^- = 34\ TbFe_3 + 33\ O^{2-} \quad (1.19)$$

$$4\ TbFe_3 + Tb_2O_3 + 6\ e^- = 6\ TbFe_2 + 3\ O^{2-} \quad (1.20)$$

In the same study (Qiu et al. 2006) the authors have shown the importance of sintering temperature. After deoxidation, the pellet sintered at 1200°C converts to $TbFe_2$ completely as desired. Reduction of the pellet sintered at 800°C on the other hand, yields $TbFe_2$ and other intermetallic compounds between Tb and Fe which were undesirable. According to their explanation, sintering at higher

temperatures results in better mixing of Tb and Fe in the atomic level and therefore yields the desired composition ($TbFe_2$) as a single phase.

$TbNi_5$ was synthesized by Qiu et al. (2006). The starting materials were Tb_4O_7 and NiO. These powders were pressed and then sintered at 1000°C. The electrolysis was carried out in pure anhydrous $CaCl_2$ at 850°C. Different constant voltages were applied during experiments in the range 0.5-3.2 V. The duration of the experiments were varied from 0.5 hour to 12 hours. According to the authors complete reduction could be achieved at 3.1 V within 12 h. The authors also indicate that increasing cell voltage shortens the time needed for deoxidation, however it also decreases current efficiency and leads to higher energy consumption.

In the study made by Tan et al. (2007), FeTi was synthesized from Fe_2O_3 - TiO_2 mixture which was sintered at 1000°C. Molten $CaCl_2$ electrolyte was used as electrolyte and the reduction temperature was 900°C. The voltage applied was constant at 3.2V and the final product was confirmed to be FeTi after electrolysis.

2.4 Electrolytes for Electrodeoxidation

The main function of the electrolyte in the electrodeoxidation process is to act as a medium for oxygen ion diffusion and therefore provide the ionic conduction in the cell which is essential for the process. The criteria for the salt selection is that it should be stable at the applied voltages, should dissolve sufficient amount of oxygen and obviously should be in the liquid state at the temperature of operation.

The molten salt used in most of the studies is $CaCl_2$ (Chen et al. 2000, Schwandt et al. 2005, Gordo et al. 2004, Glowacki et al. 2003, Jin et al. 2004) whereas in some studies $BaCl_2$ is also mentioned (Gordo et al. 2004). Gordo et al. (2004)

states the reasons for using $CaCl_2$ as its low cost, non-toxicity, availability, capability of dissolving oxygen ions but incapability of dissolving the metal oxide. $CaCl_2$ melts at 772°C, thus the electrolysis involving pure $CaCl_2$ are generally performed at temperatures higher than 772 °C typically between 850°C-900°C. This condition necessitates that only high melting point oxides could be reduced in $CaCl_2$. Examples include TiO_2 (Chen et al. 2000) ($T_{melting}$ = 1870°C), Nb_2O_5 (Yan and Fray 2002) ($T_{melting}$ = 1512°C), Cr_2O_3 (Gordo et al. 2004) ($T_{melting}$ = 2435°C), SnO_2 (Glowacki et al. 2003) ($T_{melting}$ = 1127°C) and NiO (Tan et al. 2007) ($T_{melting}$ = 1984°C).

Where low melting point oxides are involved, the electrodeoxidation could still be carried out in the solid state by lowering the electrolysis temperatures. If necessary, instead of $CaCl_2$, the eutectic mixture of $CaCl_2$ with NaCl which has a melting point of 504°C could be made use of. In fact equimolar mixture of NaCl and $CaCl_2$ have been used for electrodeoxidation of Nb_2O_5, Cr_2O_3, SnO_2 (Yan and Fray 2002, Gordo et al. 2004, Glowacki et al. 2003). However there are oxides which has melting point less than 504°C such as B_2O_3. Further decrease in the electrolysis temperature could be achieved by making use of other chlorides (KCl, LiCl, Fe_3Cl, etc.). But the limited oxygen solubility of these chlorides restricts their use as electrolyte for this method. Another drawback in lowering the temperature of deoxidation is the reduced reduction rate of the electrolysis.

A few studies so far, are available with the reaction product involved (metal or alloy) being liquid at the process temperature. Gallium in Ni_2MnGa in the study of Muir Wood et al. (2003) and tin in Nb_3Sn in the study of Glowacki et al. (2003) have melting points well below the temperature of reduction. Tin has a melting point at 232°C and that of gallium is 30°C whereas the reduction temperature was 900°C in both cases. Normally these metals were to melt as soon as they are reduced and dissipate the electrolyte. However there are no reported losses of these elements in these two studies. This may be due to the rapid reaction of the

reduced metal with the other elements (Ni, Mn, and Nb) in the cathode forming the intermetallic compounds.

However, there are currently no studies that involve an oxide that has a melting point lower than that of the molten salt. In such conditions the oxide would be expected to melt at the onset of the electrolysis.

2.5 Properties of B_2O_3 and Fe_2O_3

B_2O_3 is a white, glassy solid also known as diboron trioxide. It is almost always found as the amorphous form; however, it can be crystallized after extensive annealing into rhombohedral or monoclinic crystal system. Boron oxide has no melting point, but a vitrification range starting from 450°C (Lide 1998).

Iron (III) oxide — also known as ferric oxide, hematite— is one of the several oxide compounds of iron, and hexagonal or rhombohedral crystal structure. It has a melting point of 1565 °C.

Figures 3 and 4 show the phase diagrams of B_2O_3-Fe_2O_3 and B-Fe systems respectively. From the diagram of B_2O_3-Fe_2O_3 it is seen that the system contains two compounds, Fe_3BO_6 and $FeBO_3$. Also apparent from the diagram is that the melting point of $FeBO_3$ is around 850°C and melting point of Fe_3BO_6 is 900°C. For the Fe-B system iron rich Fe_2B compound remains solid up to 1935°C whereas FeB melts at around 2196°C.

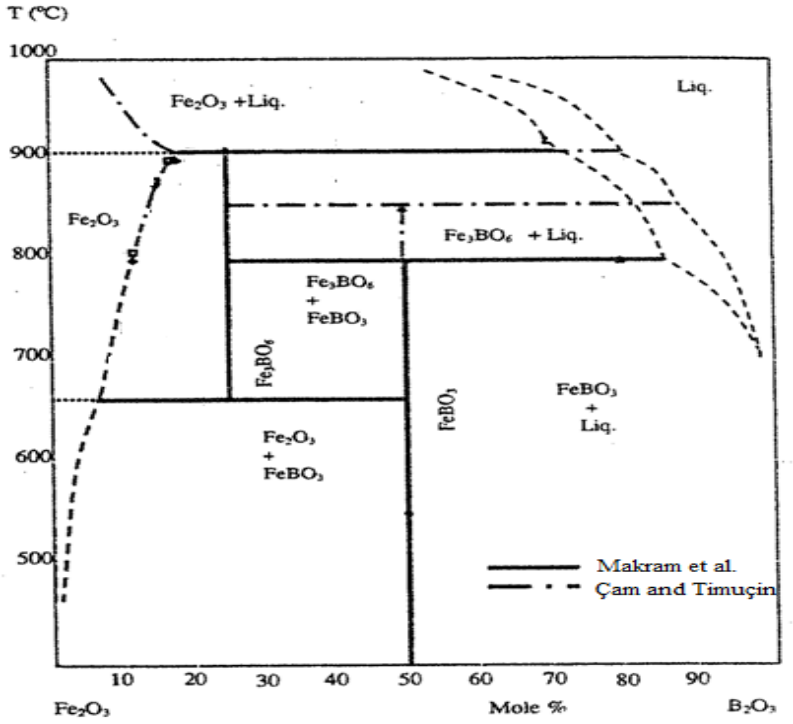

Figure 3: B_2O_3-Fe_2O_3 phase diagram (Makram et al. 1972 modified by Çam and Timuçin 2004)

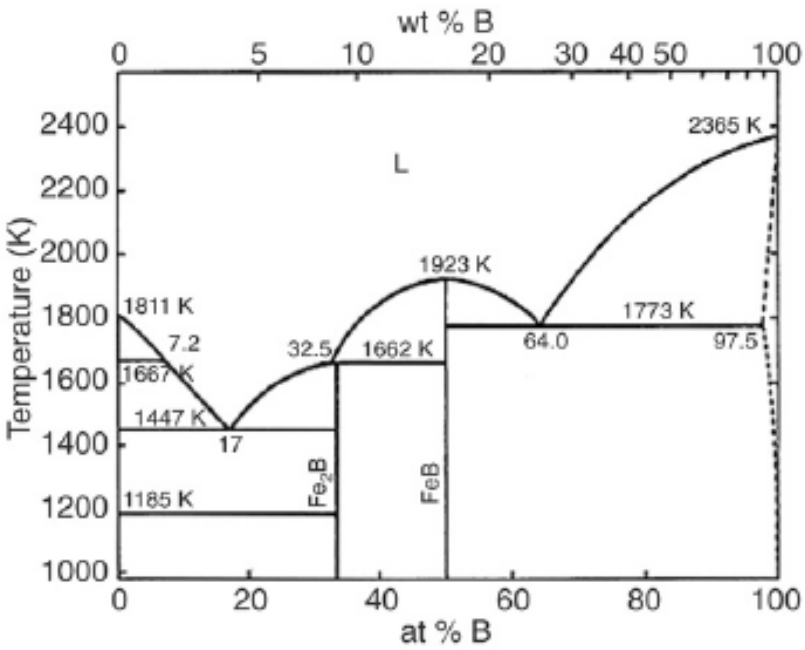

Figure 4: B-Fe phase diagram (from Massalski 1990)

CHAPTER 3

EXPERIMENTAL

3.1 Materials and Sample Preparation

Starting powders were Fe_2O_3 and H_3BO_3 both of technical grade. Powders were mixed in atomic proportions corresponding to Fe_2O_3 - 20 % B_2O_3, Fe_2O_3 - 33.3 % B_2O_3, Fe_2O_3 -50 % $B_2O_3$and Fe_2O_3 - 64 % B_2O_3. The powders were mixed together for 2 hours in a spex mill with a ball-to-powder ratio of 1.5. The mixture was then pressed under 110 MPa by a hydraulic press to form cylindrical pellets of 15 mm in diameter each weighing approximately 2 grams.

The pellets produced were sintered at 900°C under normal atmosphere in a vertical tube furnace. The heating rate was kept slow (5 $^{\circ}$C /min) so as to let the boric acid release its water, and convert to B_2O_3. Since the as-pressed compact was porous, it is considered that the water could be released quite easily, in the process creating a more porous structure.

For the experiments on samples containing CaO technical grade CaO was heated to 950°C (to release CO_2 and H_2O from possible $CaCO_3$ and $Ca(OH)_2$ compounds) and then mixed with H_3BO_3 to obtain $Ca_3B_2O_6$ by heating the mixture to 900°C for 4 hours.

Technical grade $CaCl_2$ was used in the experiments. In each experiment, 1 kg of hydrous $CaCl_2$ was used as the starting chemical for the electrolyte. Upon heating, the chemical lost most of its H_2O content and became anhydrous $CaCl_2$.

3.2 Electrochemical Cell

The electrodeoxidation experiments were carried out in an electrochemical cell shown in Figure 5. The cell comprises a stainless steel crucible that contains the electrolyte, one anode (graphite), one cathode (metal oxide) and another cathode used solely for pre-electrolysis step. All were enclosed in a stainless steel container which was maintained under Ar gas (99.995 % purity) flow at a rate of approximately 200 ml/min.

The reactor was placed in a vertical tube furnace with 160 mm in diameter and 350 mm in height. The furnace was heated with Kanthal wire wound around the tube. The temperature of the furnace was controlled +- 10 $^{\circ}C$ by Honeywell DC1010 temperature controller.

3.3 Pre-electrolysis

Prior to the electrodeoxidation of the samples, a pre-electrolysis step was applied. The reason in doing so was to remove the physically or chemically bound water and other dissolved impurities (e.g. Fe_2O_3, CaO and impurities in as received $CaCl_2$, such as sodium and sulfates). Pre-electrolysis was carried out by dipping stainless steel cathode and graphite anode to the molten salt and applying a voltage of 3.0 V. The pre-electrolysis was carried for all samples at 850 °C for 8 hours.

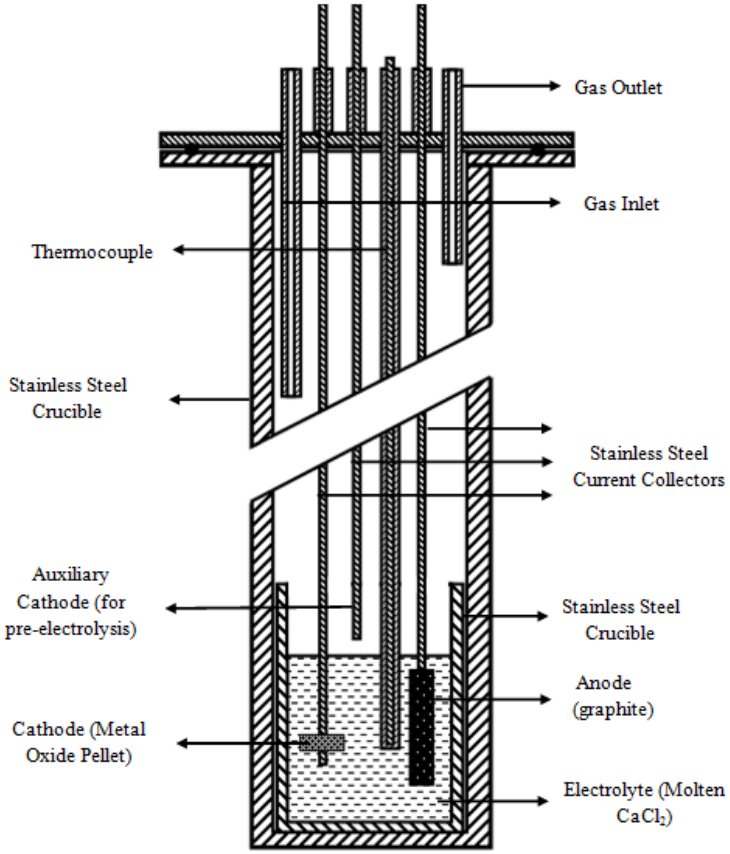

(a)

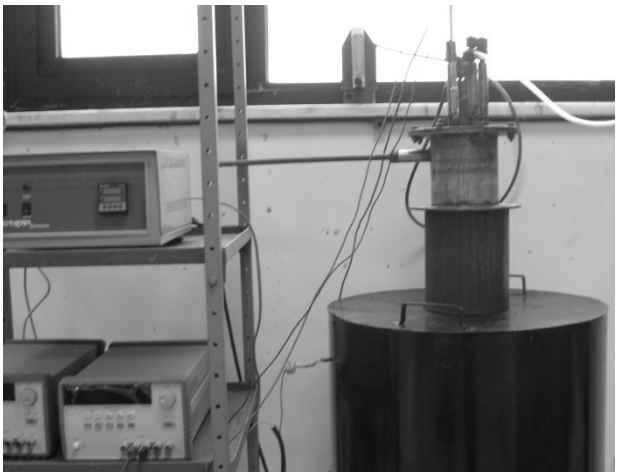

(b)

Figure 5: (a) Schematic view of the electrolysis cell, (b) Photograph showing the complete set-up

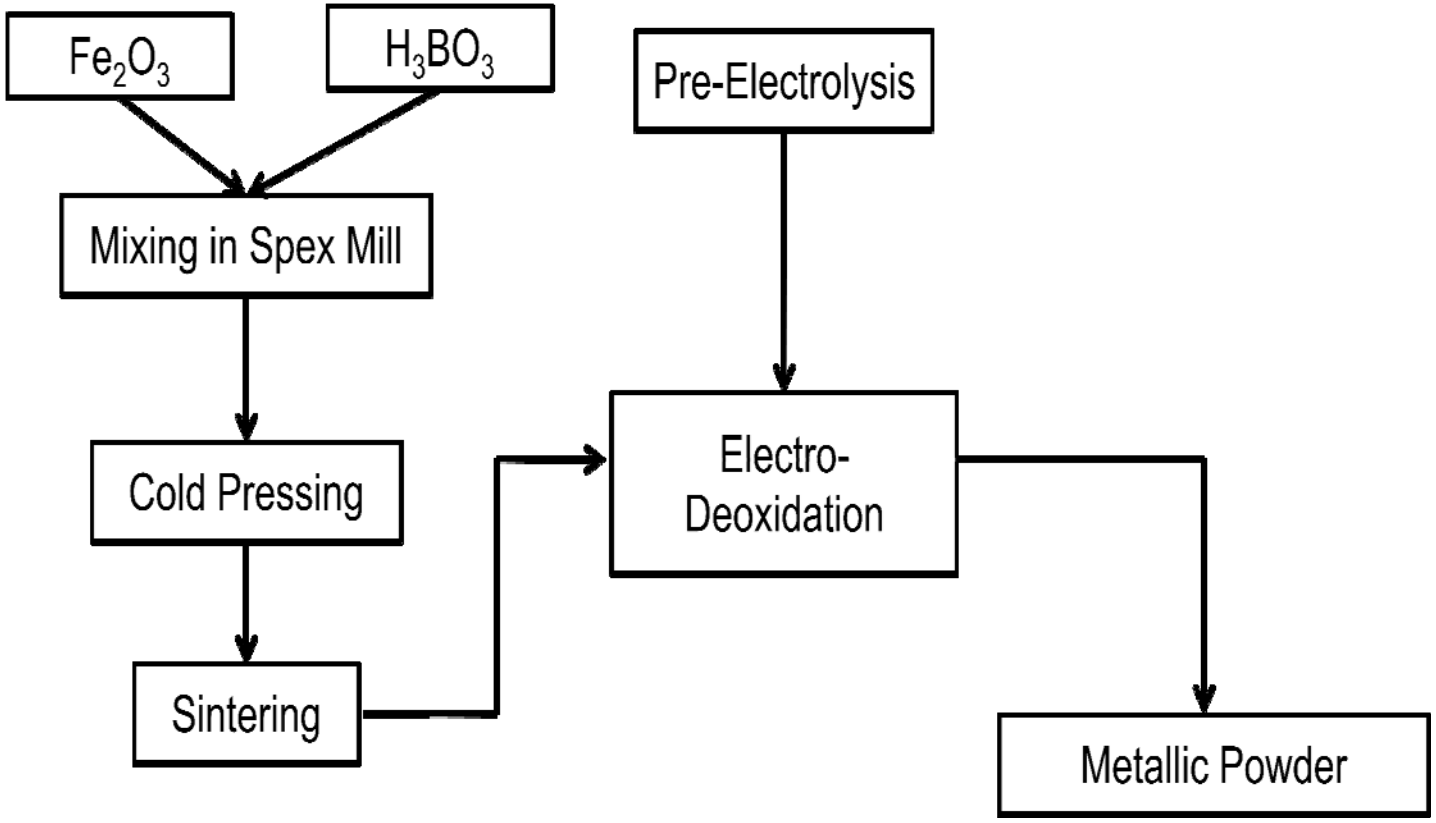

Figure 6: Sample preparation for electrodeoxidation of Fe_2O_3 and B_2O_3 mixture (left hand side of the diagram) with deoxidation steps and subsequent product

3.4 Electrodeoxidation

Upon finishing pre-electrolysis, stainless steel cathode was lifted from the salt and the other cathode holding the oxide pellet maintained inside the reactor was lowered into the salt bath. The electrolysis was carried out at a constant potential of 3.1 V All experiments were carried out at 850 °C, and the current vs. time graphs were recorded.

After the electrolysis, the electrode was lifted above the electrolyte and left to cool to room temperature inside the reactor under Ar atmosphere. Once cooled to room temperature, the samples were removed from the reactor, washed in water, dried in a drying cabinet at 100 °C, crushed and powdered with the use of mortar.

Schematic representation of the sample preparation and deoxidation experiments is given in Figure 6.

CHAPTER 4

RESULTS AND DISCUSSION

4.1 Characterization of Sintered Samples

The oxide mixtures having molecular ratio of Fe_2O_3: B_2O_3 = 4:1, 2:1, 1:1, 1:2 were sintered at 900°C. Compositions which were rich in B_2O_3 have all partially melted or lost their shape during sintering. As a result only the sample with Fe_2O_3: B_2O_3 = 4:1 could be sintered successfully.

X-ray pattern of the sample Fe_2O_3: B_2O_3 = 4:1 sintered at 900 °C for one hour and two hour durations are given Figs 7a and 7b respectively. The pellet sintered for 1 hour contains only the Fe_2O_3 phase. There is no evidence of B_2O_3 phase in this structure. This may due to B_2O_3 being in glassy phase which cannot be detected by x-rays.

X-ray pattern of the sample sintered for 2 hours yielded a new phase. This was Fe_3BO_6 which coexisted with Fe_2O_3 as would be expected from the Fe_2O_3 - B_2O_3 phase diagram. The phase Fe_3BO_6 remains solid up to 900°C which is very much higher than that of B_2O_3. Since the electrodeoxidation process requires that the oxide pellet be solid throughout the reduction process - so as to keep the electrical contact between the cathodic current collector (stainless steel wire) and the oxide

phases at all times- the formation of this phase would ease the reduction process. As a result; the sintering conditions were fixed as 2 hours at 900°C.

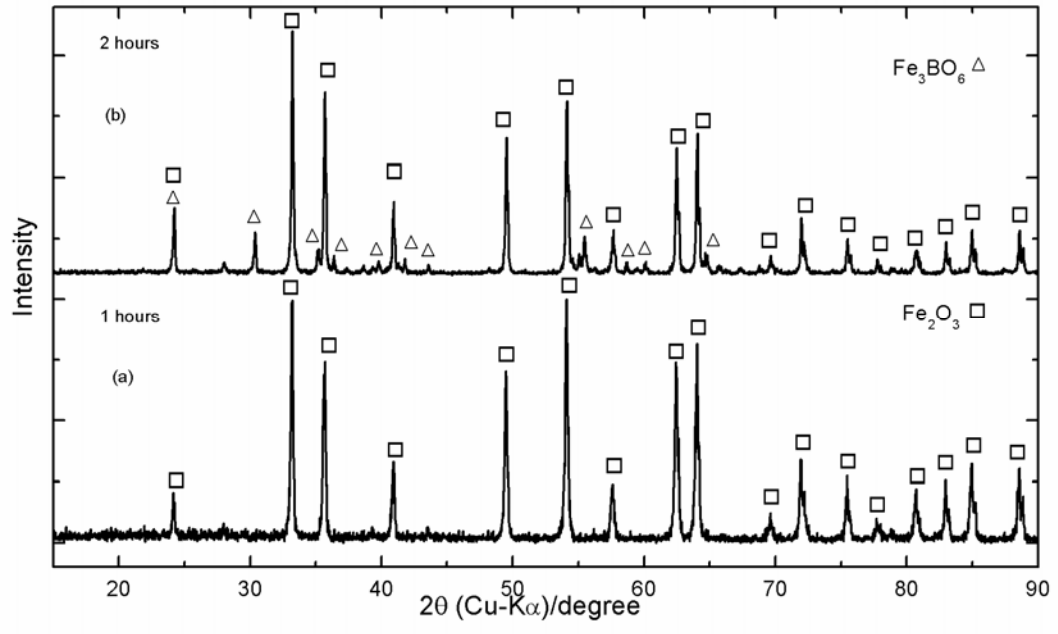

Figure 7: X-ray spectrum of Fe_2O_3 - 20 at % B_2O_3 mixture sintered at 900°C for a) 1 hour and b) 2 hours

SEM image of the pellet Fe_2O_3: B_2O_3 = 4:1 sintered for 2 hours at 900°C is given in Figure 8a. The image shows a highly porous structure. Porosities calculated from the apparent densities of the constituent phases are about 41 %.

4.2 Electrodeoxidation of Fe_2O_3 - B_2O_3 mixture

Electrodeoxidation experiments were carried out for Fe_2O_3: B_2O_3 = 4:1 mixture only. Attempts to deoxidize the other compositions, i.e. Fe_2O_3: B_2O_3 = 2:1, 1:1, 1:2 have failed since the pellets have disintegrated in the electrolyte probably due to melting of the B_2O_3 phase.

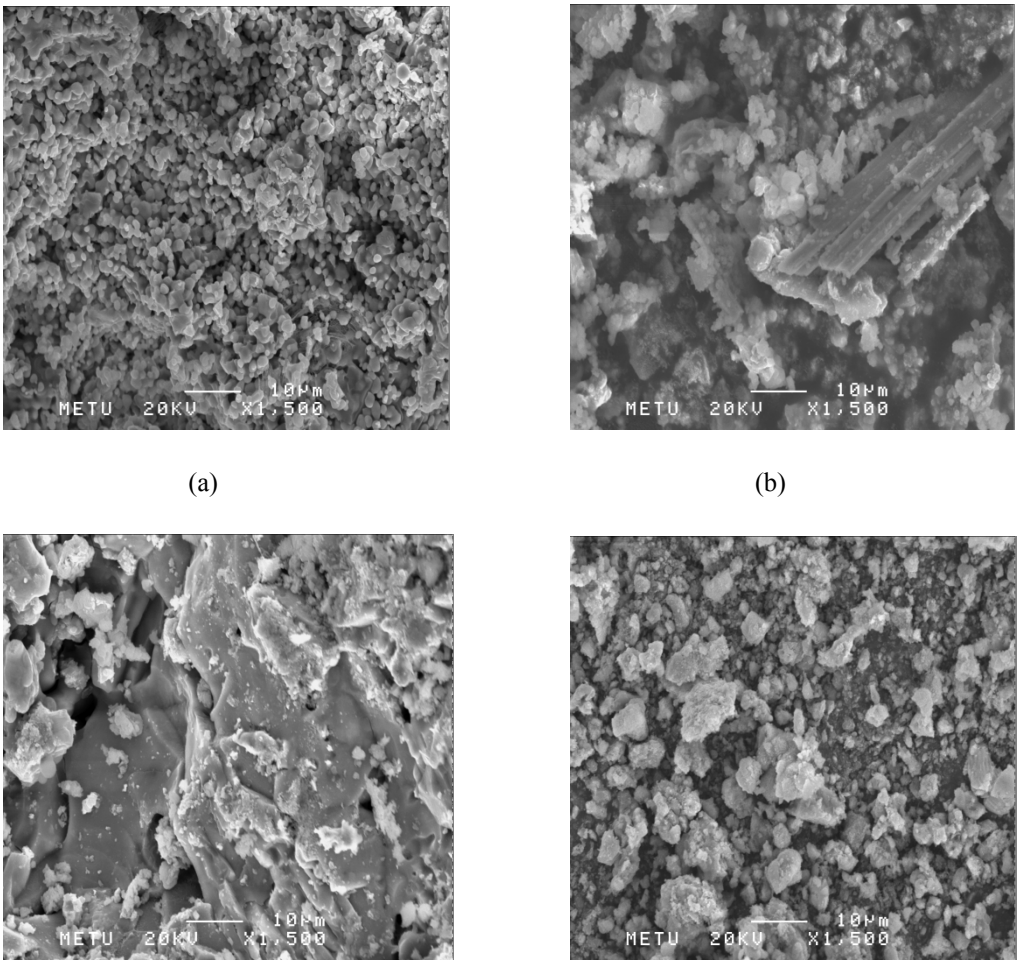

(a) (b)

(c) (d)

Figure 8: SEM images of a) Fe_2O_3 - 20 at % B_2O_3 compact sintered at 900°C for 2hours, electrodeoxidized in molten $CaCl_2$ at 850°C and 3.1 V; b) for 0.5 h, c) for 3 h, d) for 12 h

The current-time plot recorded for Fe_2O_3: B_2O_3 = 4:1 pellet is given in Figure 9. As seen in the Figure, within a short period the current rises to a high value and then decreases sharply and then gradually cascades down to smaller values finally settling at 0.5 A.

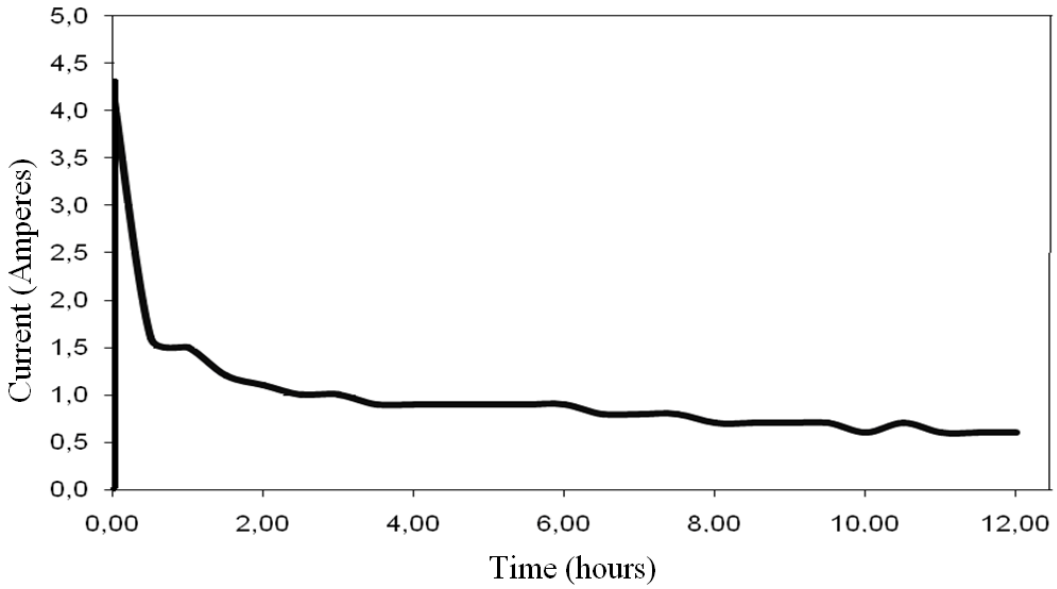

Figure 9: Current (A) vs. Time (hours) plot recorded during 12 hour electrodeoxidation

X-ray pattern of the sample reduced for 12 hours is given in Figure 10d. As seen in this Figure the pattern contains two phases Fe and Fe_2B. There is no trace of any oxide compounds or unreacted boron. This shows that during 12 hours of electrodeoxidation the sample has not only been fully reduced but also elemental Fe and B have reacted to form the Fe_2B which would be expected according to the

relevant phase diagram (see Figure 4). SEM image of the powder as obtained after 12 hours of deoxidation is given in Figure 8d.

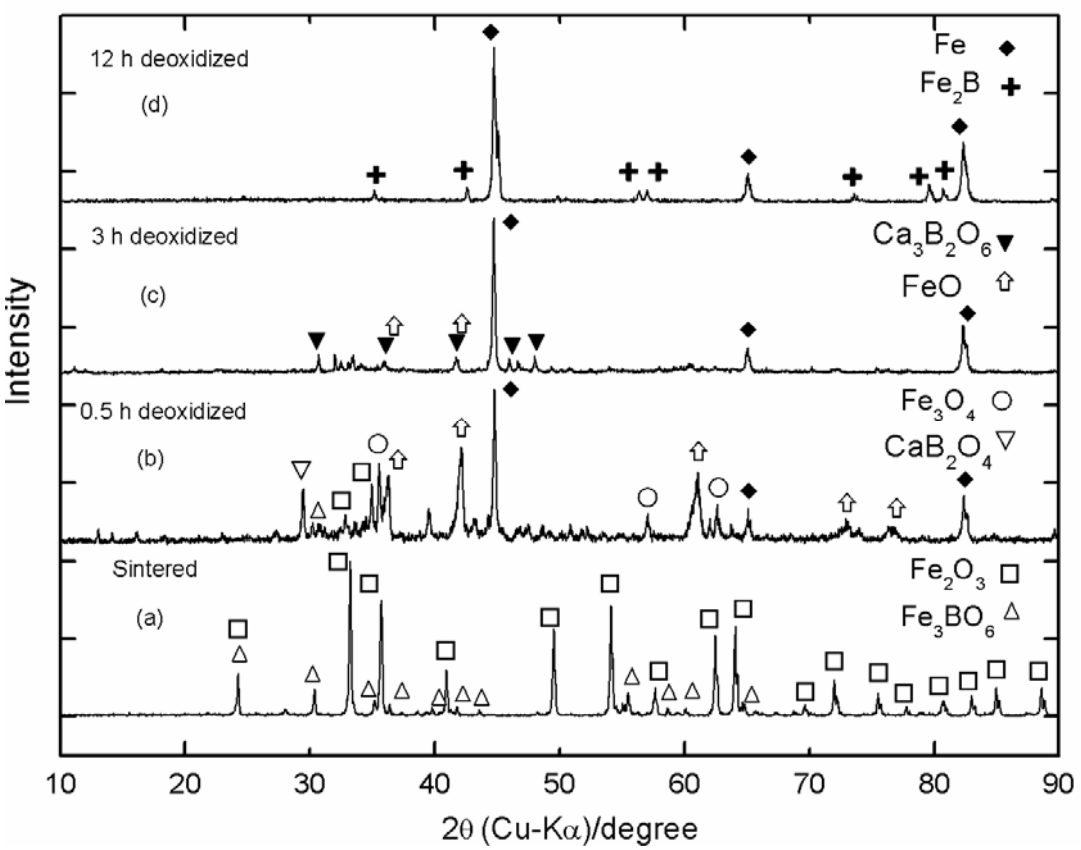

Figure 10: X-ray spectra of Fe_2O_3 - 20 at % B_2O_3 pellet a) as -sintered condition (900°C for 2 hours). Sintered pellet deoxidized at 850°C and 3.1 V for b) 0.5 hours, c) 3 hours and d) 12 hours

Quantities of phases as calculated from X-ray data for the reduced sample give a weight percentage value of 34 % for Fe_2B. This corresponds to a composition of Fe - 14 at% B which is on the iron rich side of the eutectic composition. Since the original mixture was prepared for Fe - 20 at% B, there is some loss of boron content during the reduction.

The sequence of changes that occur during the reduction process was examined by interrupted experiments for durations that are shorter than 12 hours. These durations were chosen based on the current-time graph as 0.5 hours and 3 hours.

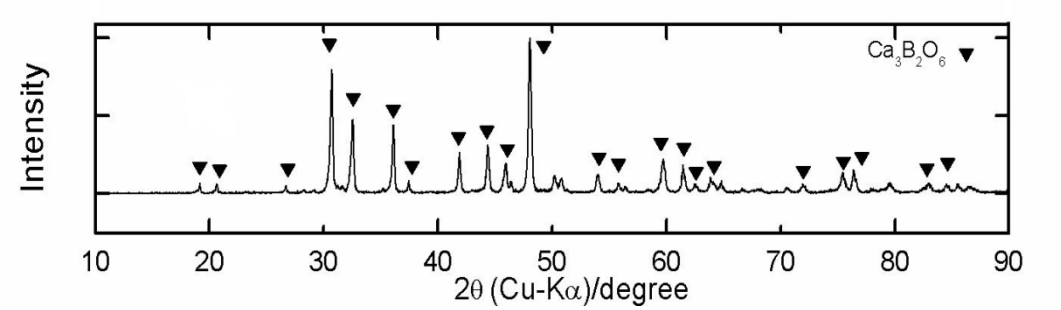

Figure 11: X-ray spectrum of $Ca_3B_2O_6$ synthesized by mixing and sintering of CaO and B_2O_3 in molecular ratio of 3:1

The sample closest to the one reduced for 12 hours is the one that has been electrolyzed for 3 hours. SEM images taken from the sample are given in Figure 8c. X-ray pattern of this sample shown in Figure 10c, comprises Fe as the dominant phase. FeO was also present in the sample probably derived from partial deoxidation of Fe_2O_3. The sample does contain other phases that are difficult to identify. Calcium borate; $Ca_3B_2O_6$ appear to be present but needs to be verified. So as to ascertain the presence of this phase, a sample was prepared by mixing CaO and B_2O_3 in the molecular ratio of 3:1 which was then sintered for 4 hours at 900 $^{\circ}$C. X-ray diffractogram of this sample is given in Figure 11. It is seen that the phases reacted with each other giving a single phase oxide which matches calcium borate. The peak positions in Figure 11 do match with most of the remaining peaks in Figure 10c which refers to the 3 hour deoxidized sample. Thus it can be concluded that the chemical pathway of electrodeoxidation do involve the formation of calcium borate. This phase probably formed by the reaction of B_2O_3

with CaO, which is normally present in $CaCl_2$ as it forms during the drying process*, by the reaction of $CaCl_2$ and H_2O, giving rise to the formation of calcium borate. Similar formation do occur in other systems e.g. calcium titanate formation in the deoxidation of TiO_2. (Schwandt et al. 2005)

An interesting observation with regard to 3 hour deoxidized sample is that iron boron compounds have not yet formed in the sample. This shows that boron reduction occurs quite late in the process in the time bracket between 3 to 12 hours. Whether or not the current sample contain pure boron cannot be stated directly since boron can be in amorphous state and can therefore escape detection by X-rays. To check the stoichiometry of the boron, a quantitative phase analysis was carried out via Rietveld refinement of X-ray diffractogrammes. This yielded values of 47, 33, 20 wt % for Fe, calcium borate, and FeO respectively. This corresponds to Fe:B ratio of 3.97:1 which is quite close to the original value 4:1. This implies that all boron is tied up in calcium borate in the sample and has not yet been reduced to elemental state.

X-ray diffractogram of the sample electrodeoxidized for 30 minutes show that iron is already a substantial phase. This verifies the observation made above that iron forms quite early in the process. The other phases present are FeO, Fe_3O_4 and possibly a Ca bearing phase namely CaB_2O_4. Traces of Fe_2O_3 and Fe_3BO_6 which make up the sintered pellet could also be detected (compare (a) with (b) in Figure 10). It is interesting to note that within 30 minutes there is a drastic diminution of Fe_3BO_6 phase. This probably occurs due to the reaction of this phase with CaO forming calcium borate. SEM image taken from the sample is shown in Figure 8b.

* $CaCl_2$ (s) + H_2O (l) = CaO (s) + 2 HCl (g)

4.3 Chemical Pathway of Deoxidation in Fe_2O_3 - B_2O_3 systems

The experimental findings discussed so far should be in accordance with the thermodynamic explanation of the behavior of the mentioned phases and species. However, lack of thermodynamic and kinetic data and (overpotentials in the system, solubility behaviors, free energies of formation, etc.) as well as difficulties in characterization of reactions and phases especially in the intermediate stages of the reduction process hinders the proposal of a deterministic mechanism for the electrodeoxidation of Fe_2O_3 - B_2O_3 mixture in molten $CaCl_2$. Instead, a brief discussion relying mainly on x-ray results and available thermodynamic data will be given here in order to describe general pathway for reduction. Thermodynamic data for the calculation of Gibbs free energies and standard potentials were obtained from http://www.crct.polymtl.ca/fact/ and Barin et al. 1973.

One of the key phases for the purpose of this discussion is Fe_3BO_6. There is no thermodynamic data readily available for the standard Gibbs free energy of formation of the Fe_3BO_6 that can be obtained from the mentioned databases. Therefore, for the sake of further discussion, the standard Gibbs free energy of formation of the Fe_3BO_6 is calculated from the thermodynamic data and phase diagram of Fe_2O_3 -B_2O_3 available at http://www.crct.polymtl.ca/fact/. Details of this calculation are given in Appendix.

$$3\ Fe\ (s) + B\ (s) + 3\ O_2\ (g) = Fe_3BO_6\ (s)\ \Delta G^\circ = -\ 1310\ kJ \qquad (4.1)$$

It appears that there are systematic changes in the sintered pellet during deoxidation. The initial structure comprising Fe_2O_3 and Fe_3BO_6 phases are subject to early modification possibly due to reaction with CaO. This probably occurs via

$2\ Fe_3BO_6\ (s) + CaO\ (s) = 3\ Fe_2O_3\ (s) + CaB_2O_4\ (s)$ $\Delta G°$=-68.1 kJ (4.2)

or

$2\ Fe_3BO_6(s) + 3\ CaO\ (s) = 3Fe_2O_3\ (s) + Ca_3B_2O_6\ (s)$ $\Delta G°$= -86.1 kJ (4.3)

Thus it appears that the reduction process proceeds with Fe_2O_3 and calcium borate. Possible reactions with which the reductions occur are shown below. Using the thermodynamic data, the decomposition voltages of the various oxides have been calculated and listed below in descending order. The values here were determined for the reactions taking place at 850°C. CO is assumed as the only anodic gas because the Boudouard reaction predicts $CO:CO_2$ ratio as 9:1 at 850°C.

$Fe_2O_3\ (s) + 1/3\ C\ (s) = 2/3\ Fe_3O_4\ (s) + 1/3\ CO\ (g)$ $E° = 0.41$ V (4.4)

$2/3\ Fe_3O_4\ (s) + 2/3\ C\ (s) = 2\ FeO\ (s) + 2/3\ CO\ (g)$ $E° = 0.22$ V (4.5)

$2\ FeO\ (s) + 2\ C\ (s) = 2\ Fe\ (s) + 2\ CO\ (g)$ $E° = 0.09$ V (4.6)

$2\ Fe_3BO_6\ (s) + 3\ C\ (s) = 3\ Fe_2O_3\ (s) + 2\ B\ (s) + 3\ CO\ (g)$ $E° = -0.01$ V (4.7)

$B_2O_3\ (l) + 3\ C\ (s) = 2\ B\ (s) + 3\ CO\ (g)$ $E°$= -0.62 V (4.8)

$CaB_2O_4\ (s) + 3\ C\ (s) = 2\ B\ (s) + CaO\ (s) + 3\ CO\ (g)$ $E°$= -0.79 V (4.9)

$Ca_3B_2O_6$ (s) + 3 C (s) = 2 B(s) + 3 CaO(s) + 3 CO (g) E° = -1.63 V (4.10)

It should be noted that the reactions involving iron oxides, i.e. reactions (4.4)-(4.6) have positive values implying that these reactions are spontaneous and therefore should occur more easily. This is consistent with the fact that iron is extracted quite early in the process. It should also be noted that the values of decomposition voltage for boron bearing oxides are very much lower than those of iron oxide. This is particularly true for $Ca_3B_2O_6$ where the value is E°=-1.63 V. Thus boron bearing oxides are more difficult to reduce. This is probably the reason for the late appearance of boron bearing metallic compounds in the current experiments. It is worth noting that the value of decomposition voltages for calcium borates are even lower than that of B_2O_3 and Fe_3BO_6, compare reactions (4.7), (4.8) with reactions (4.9), (4.10).

The Fe_2B compound in the final alloy is produced via the following spontaneous reaction:

2 Fe (s) + B (s) = Fe_2B (s) $\Delta G°$ = -66.6 kJ (4.11)

As indicated earlier there is a loss in boron content in the produced alloy. This is attributed to the melting of B_2O_3. Since the details of the reduction path are unclear it is not possible to show the step responsible for the boron loss. Two possible reactions that could cause boron loss are as such:

2 Fe_3BO_6 (s) = 3 Fe_2O_3 (s) + B_2O_3 (l) $\Delta G°$= 26.4 kJ (4.12)

$Ca_3B_2O_6$ (s) = 3 <u>CaO</u> (in $CaCl_2$) + B_2O_3 (l) (4.13)

The reaction (4.12), although not spontaneous at 850°C, could be shifted forward by the decrease in Fe_2O_3 content due to its reduction. The reaction (4.13) is more probable because findings of 3 hour reduction showed that all of the starting

boron content converts to $Ca_3B_2O_6$. Reaction (4.13) could be shifted to the product side by lowering the activity of CaO dissolved in $CaCl_2$. The possible electrolysis of this dissolved CaO may lower the CaO activity and cause boron loss in the final alloy.

Results reported above show that Fe_2O_3-B_2O_3 oxide mixture can be reduced quite successfully in molten $CaCl_2$. The fact that B_2O_3 is liquid at the electrolysis temperature did not affect the deoxidation process simply because reacting with Fe_2O_3 it formed a high melting point oxide phase; Fe_3BO_6. The formation of this phase is quite beneficial in this respect. B_2O_3 – Fe_2O_3 phase diagram (see Figure 4) implies that Fe-B alloys up to 25 at % B can be synthesized using the current approach without the risk of melting in the cathode. The results further show that Fe_3BO_6 is subject to early decomposition. This probably occurs due to its reaction with CaO, which is always present in $CaCl_2$ during the drying process. It appears that this reaction, as shown above, leads to formation of calcium borate which again has a high melting point (approximately 1475°C).

CHAPTER 5

CONCLUSION

In the current work, Fe -20 at % B alloy was synthesized from their oxides via electrodeoxidation in molten $CaCl_2$. The oxides; Fe_2O_3 and B_2O_3 mixed in suitable proportions were sintered at 900 °C yielding pellets with a two-phase structure; Fe_2O_3 and Fe_3BO_6. The sintered pellets connected as cathode were then electrodeoxidized in molten $CaCl_2$ (850°C) using graphite anode at 3.1 V. The electrolysis of the mixed oxide pellet for duration 12 hours successfully yielded the target composition in the form of a powder mixture of Fe and Fe_2B.

The sequence of changes that occur in the pellet during the electrolysis was studied using the interrupted experiments. The reduction of iron occurs quite early in the process through the depletion of oxygen from the starting oxide Fe_2O_3, forming other iron oxides in the process. Boron initially contained in Fe_3BO_6 has followed a different route. The reduction occurs from calcium borate, an intermediate phase formed after the depletion of Fe_3BO_6. Boron is therefore extracted late in the process and seems to react with iron, forming the compound Fe_2B.

Future work on the subject may involve a more detailed characterization of the reduction procedure in order to determine the steps causing the boron loss. Crystallization behavior of the alloy could be investigated to confirm that the

product is fully suited to amorphous ferroboron production. Possibilities of large scale ferroboron production should be assessed.

REFERENCES

Akdeniz, M. V., Mekhrabov, A. O., Pehlivanoglu, M. K., *J Alloys Comp.,* **vol. 386** (2005), p. 185-191.

Barin I., Knacke O., Kubaschewski O., Thermochemical Properties of Inorganic Substances, 2nd ed., Springer-Verlag, Berlin, (1973).

Çam İ. and Timuçin M., *2nd Int. Boron Symp*, Eskişehir (2004).

Chen, G. Z. and Fray D. J., *J. Electrochem. Soc.,* **vol. 149** (2002), p. E455-E467.

Chen, G. Z., Fray, D. J., & Farthing, T. W. *Nature,* **vol. 407** (2000), p. 361-364.

Collection of Phase Diagrams, [http://www.crct.polymtl.ca/fact/] Last Accessed: June 2008.

Deng Y., Wang D., Xiao W., Jin X., Hu X. and Chen G.Z. *J. Phys. Chem.* B, **vol. 109** (2005), p. 14043-14051.

FACT – Facility for the Analysis of Chemical Thermodynamics, [http://www.crct.polymtl.ca/fact/], Last Accessed: July 2008.

Fray D.J. and Chen G.Z., *Mater. Sci. Tech.,* **vol. 20** (2004), p. 295-300.

Fray, D.J., Farthing, T.W. and Chen, G. Z. Inter. Pub. No. WO9964638.

Glowacki, B.A., Fray, D.J., Yan, X-Y. , Chen, G. Z. *Physica C,* **vol. 387** (2003), p. 242-246.

Gordo, E., Chen, G. Z., Fray, D. J., *Electrochim. Acta,* **vol. 49** (2004), p. 2195-2208.

Inoue A. Zhang T., Itoi T., Takeuchi A., *Mat. Trans., JIM,* **vol. 38** (1997), p. 359.

Jin X., Gao P., Wang D., Hu X. and Chen G.Z., *Angew. Chem. Int. Ed.,* **vol. 43** (2004), p. 733-736.

Lide D.R., Ed. CRC Handbook of Chemistry and Physics, 79th Edition, CRC Press, Boca Raton, FL (1998).

Makram H., Touron L., Loriers J., *J Cryst Growth,* **vol. 13-14** (1972), p. 585

Martini C., Palombarini G., Poli G., Prandstraller D., *Wear,* **vol. 256** (2004), p. 608-613.

Massalski T.B. (Ed.), Binary Alloys Phase Diagrams, 2nd edition, ASM International, Metals Park, OH, (1990).

McHenry M. E., Willard M. A., Laughlin D. E., *Prog. Mater. Sci.,* **vol. 44** (1999), p. 291.

Mohandas, K.S. and Fray D.J., *Trans. Indian Inst. Met.,* **vol. 57** (2004), p. 579-592.

Muir Wood, A.J., Copcutt, R.C., Chen, G.Z. & Fray, D.J., *Adv. Eng. Mater.,* **vol. 5**, (2003), p. 650-653.

Nilsson, O., Sandberg, O. and Bäckström, G., *Inter. J. Thermophys.,* **vol. 6** (1985), p. 267-273.

Okabe T.H., Oishi T., Ono K., *J Alloy Comp.,* **vol. 184** (1992), p. 43-56.

Qiu G., Wang D., Jin X. and Chen G.Z., *Electrochim. Acta,* **vol. 51** (2006), p. 5785-5793.

Qiu G., Wang D., Ma M., Jin X. and Chen G.Z., *J Electroanal. Chem.,* **vol. 589** (2006), p. 139-147.

Schwandt, C., Fray, D.J. *Electrochim. Acta,* **vol. 51**, (2005), p. 66-76.

Tan S., Örs T., Akyıldız H., Kalcıoğlu A. F. and Öztürk T, *2nd Int. Hydrogen Energy Congress,* Istanbul (2007).

Tan S., Ozturk T., Aydinol M.K., and Karakaya I., *211th Elecrochem. Soc. Meeting,* Chicago (2007).

Ward R. G., and Hoar T. P., *J. Inst. Met.*, **vol. 90** (1961), p. 6.

Yan X.Y. and Fray D.J., *Metall. and Mater. Trans. B*, **vol. 33B** (2002), p. 685-693.

Yücel, O., Çınar, F., Addemir, O., Tekin,A. *High Temp. Mater. Process.,* **vol. 15**, (1996), p. 103-109.

APPENDIX A

CALCULATION OF THERMODYNAMIC DATA FOR Fe_3BO_6

No thermodynamic data was available for the standard Gibbs free energy of formation of Fe_3BO_6 phase in standard sources such as Barin et al. 1973. This property was therefore calculated from Fe_2O_3 - B_2O_3 phase diagram, Figure A.1a, using the thermodynamic data given for Fe_2O_3 and B_2O_3 by Barin et al. 1973.

Figure A.1b refers to the section of the phase diagram at 850°C and shows G^* versus mole fraction of Fe_2O_3 for the phases present at the given temperature. Here the curve G_L^* refers to the liquid phase and is defined as:

$$G_L^* = G_m^L - (X_{Fe_2O_3}\mu_{Fe_2O_3}^{o,S} + X_{B_2O_3}\mu_{B_2O_3}^{o,S}) \qquad (A.1)$$

Here G_m^L is the integral molar Gibbs free energy of the liquid phase, $X_{Fe_2O_3}$ and $X_{B_2O_3}$ are the mole fractions of Fe_2O_3 and B_2O_3 respectively and $\mu_{Fe_2O_3}^{o,S}$ and $\mu_{B_2O_3}^{o,S}$ are the standard chemical potential of the pure solid Fe_2O_3 and B_2O_3 respectively. Thus the property G* (for the liquid as well as for the other phases) is defined as the difference between integral molar Gibbs free energy of a phase and the standard chemical potential of pure solid forms of its constituent species (Fe_2O_3 and B_2O_3 species).

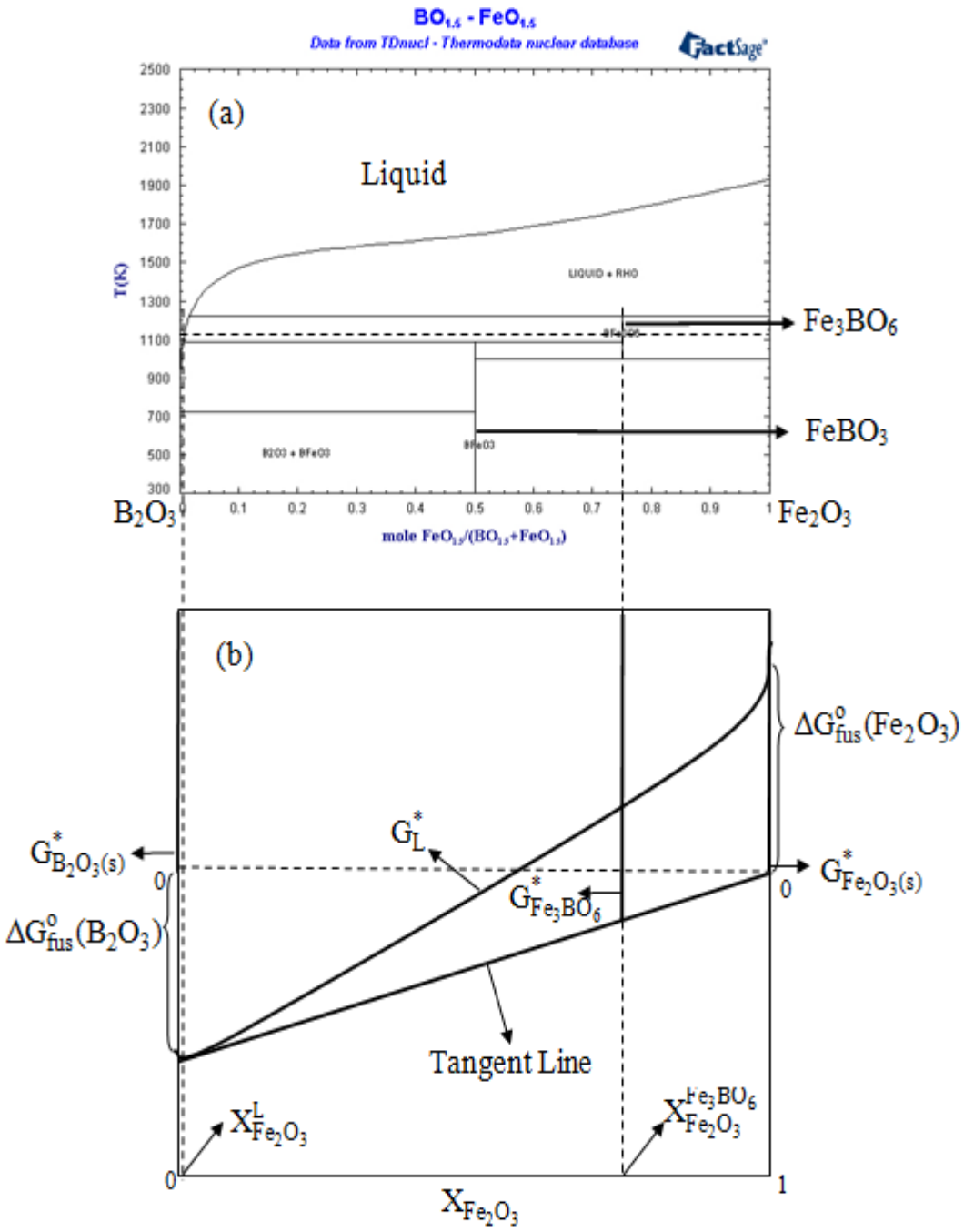

Figure A.1: Fe $_2O_3$ - B_2O_3 phase diagram (http://www.crct.polymtl.ca/fact/) and G^* curves of the phases at 850°C

The aim here is to obtain standard Gibbs free energy of formation, ΔG_f^o, for Fe_3BO_6. For this purpose, it is necessary to determine $G^*_{Fe_3BO_6}$ which is shown in Figure A.1b. As seen from the phase diagram, Fe_3BO_6 phase is in equilibrium with the liquid of liquidus composition ($X^L_{Fe_2O_3}$) and with pure Fe_2O_3 solid, i.e. $X_{Fe_2O_3}= 1$. Therefore these three phases should share a common tangent which is also shown on the diagram. To determine the value of $G^*_{Fe_3BO_6}$ it is necessary to obtain the equation of the tangent line. The value of the tangent at $X_{Fe_2O_3}= 1$ is "0" since G^* is defined relative to pure solids. Since G^*_L at $X^L_{Fe_2O_3}$ is on the tangent line, this value could be used to define the equation of the tangent line.

Thus to define the tangent it is necessary to find the value of G^*_L at $X^L_{Fe_2O_3}$. As given in equation (A.1), G^*_L is the difference between G^L_m and $(X_{Fe_2O_3}\mu^{o,S}_{Fe_2O_3} + X_{B_2O_3}\mu^{o,S}_{B_2O_3})$. Here:

$$G^L_m = X_{Fe_2O_3}\ \mu^L_{Fe_2O_3} + X_{B_2O_3}\ \mu^L_{B_2O_3} \qquad (A.2)$$

where $\mu^L_{Fe_2O_3}$ and $\mu^L_{B_2O_3}$ are the respective chemical potentials of Fe_2O_3 and B_2O_3 in the liquid phase. These chemical potentials are given by;

$$\mu^L_{Fe_2O_3} = \mu^{o,L}_{Fe_2O_3} + RT \ln a^L_{Fe_2O_3} \qquad (A.3)$$

$$\mu^L_{B_2O_3} = \mu^{o,L}_{B_2O_3} + RT \ln a^L_{B_2O_3} \qquad (A.4)$$

where $\mu^{o,L}_{Fe_2O_3}$ and $\mu^{o,L}_{B_2O_3}$ are the respective standard chemical potentials of the pure liquid Fe_2O_3 and B_2O_3; $a^L_{Fe_2O_3}$ and $a^L_{B_2O_3}$ are activities of Fe_2O_3 and B_2O_3 in the liquid phase.

Combining (A.3) and (A.4) with (A.2);

$$G^L_m = X_{Fe_2O_3}\ (\mu^{o,L}_{Fe_2O_3} + RT \ln a^L_{Fe_2O_3}) + X_{B_2O_3}\ (\mu^{o,L}_{B_2O_3} + RT \ln a^L_{B_2O_3}) \qquad (A.5)$$

Inserting (A.5) into the G_L^* definition in (A.1) and reorganizing:

$$G_L^* = X_{Fe_2O_3}\left(\mu^{o,L}_{Fe_2O_3} - \mu^{o,S}_{Fe_2O_3}\right) + X_{B_2O_3}\left(\mu^{o,L}_{B_2O_3} - \mu^{o,S}_{B_2O_3}\right)$$

$$+ RT\left(X_{Fe_2O_3} \ln a^L_{Fe_2O_3} + X_{B_2O_3} \ln a^L_{B_2O_3}\right) \qquad (A.6)$$

Noting that;

$$\mu^{o,L}_{Fe_2O_3} - \mu^{o,S}_{Fe_2O_3} = \Delta G^o_{fus}(Fe_2O_3) \qquad (A.7)$$

$$\mu^{o,L}_{B_2O_3} - \mu^{o,S}_{B_2O_3} = \Delta G^o_{fus}(B_2O_3) \qquad (A.8)$$

Finally:

$$G_L^* = X_{Fe_2O_3}\Delta G_{fus}(Fe_2O_3) + (1-X_{Fe_2O_3})\Delta G_{fus}(B_2O_3)$$

$$+RT\left[X_{Fe_2O_3} \ln a^L_{Fe_2O_3} + (1-X_{Fe_2O_3}) \ln a^L_{B_2O_3}\right] \qquad (A.9)$$

To insert the relevant values in this equation, we need to know the free energy of fusion of Fe_2O_3. However no data is available for this, since Fe_2O_3 has no real melting point (decomposes to Fe_3O_4 at elevated temperatures). Then it is necessary to calculate this value from the phase diagram. The reaction is:

$$Fe_2O_3\ (s) = Fe_2O_3\ (l) \qquad (A.10)$$

Assuming $\Delta c_p = 0$, between solid and liquid phases:

$$\Delta G^o_{fus}(Fe_2O_3) = \Delta H^o_{fus}(Fe_2O_3) - T\Delta S^o_{fus}(Fe_2O_3) \qquad (A.11)$$

Standard entropy of fusion of Fe_2O_3 is approximated by Richards rule as 2 cal/(mole K):

$$\Delta S^o_{fus}(Fe_2O_3) = 2\ \text{cal/mole K} = 8.37\ \text{J/mole K} \qquad (A.12)$$

At 1925 K, “the melting point” for Fe_2O_3 as read from the phase diagram,

$$\Delta G^{o}_{fus}(Fe_2O_3) = 0 \quad \text{(A.13)}$$

$$\Delta G^{o}_{fus}(Fe_2O_3) = 0 = \Delta H^{o}_{fus} - 8.37\times 1925 \quad \text{(A.14)}$$

$$\Delta H^{o}_{fus}(Fe_2O_3) = 16108 \ \text{J/mole} \quad \text{(A.15)}$$

Since $\Delta c_p = 0$, ΔH^{o}_{fus} and ΔS^{o}_{fus} are both independent of temperature and we can write for all T:

$$\Delta G^{o}_{fus}(Fe_2O_3) = 16108 - 8.37T \quad \text{(A.16)}$$

$$\Delta G^{o}_{fus} = -RT \ln\left(\frac{a^{L}_{Fe_2O_3}}{a^{S}_{Fe_2O_3}}\right) \quad \text{(A.17)}$$

Since Fe_2O_3 is a pure solid, $a^{S}_{Fe_2O_3} = 1$.

At the process temperature of 850°C (1123 K):

$$\Delta G^{o}_{fus}(Fe_2O_3) = 6737 \ \text{J/mole} = -RT \ln\left(a^{L}_{Fe_2O_3}\right) \quad \text{(A.18)}$$

$$a^{L}_{Fe_2O_3} = 0.486 \quad \text{(A.19)}$$

From the phase diagram $X^{L}_{Fe_2O_3}$=0.013. At this composition B_2O_3 is assumed to obey the Raoult's law. Therefore $a^{L}_{B_2O_3} = 0.987$. $\Delta G_{fus}(B_2O_3) = -13217$ J/mole (Barin et al. 1973). Inserting these values into equation (A.9);

$$G^{*}_{L} = -13166 \ \text{J/mole} \quad \text{(A.20)}$$

This value, which refers to $X^{L}_{Fe_2O_3}$, defines the tangent line. Considering the position of Fe_3BO_6 phase, i.e. $X^{Fe_3BO_6}_{Fe_2O_3} = 0.75$, on this tangent:

$$G^{*}_{Fe_3BO_6} = G^{*}_{L}\left(1-X^{Fe_3BO_6}_{Fe_2O_3}\right)/\left(1-X^{L}_{Fe_2O_3}\right) \quad \text{(A.21)}$$

Thus;

$G^{*}_{Fe_3BO_6}$= -3335 J/mole (A.22)

This quantity determined is also the standard Gibbs free energy change for the reaction:

0.75 Fe_2O_3 (s) + 0.25 B_2O_3 (s) = 0.5 Fe_3BO_6 (s) ΔG° = -3335 J (A.23)

Formation reactions of B_2O_3 and Fe_2O_3 are;

2 Fe (s) + 1.5 O_2 (g) = Fe_2O_3 (s) ΔG° = - 533566 J (A.24)

2 B(s) + 1.5 O_2 (g) = B_2O_3 (s) ΔG° = - 1005903 J (A.25)

Summing (A.23), (A.24) and (A.25) in appopriate proportions we obtain the formation reaction:

3 Fe (s) + B (s) + 3 O_2 (g) = Fe_3BO_6 (s) ΔG°= - 1309971 J (A.26)

Thus standard Gibbs free energy of formation of $Fe3BO_6$ is - 1309971 J.